Eur. J. Mineral.
1999, **11**, 23-32

High-temperature Raman spectroscopic study of H_2O-CO_2-CH_4 mixtures in synthetic fluid inclusions: first insights on molecular interactions and analytical implications

JEAN DUBESSY[1], ALAIN MOISSETTE[1]*, RONALD J. BAKKER[1], JOHN D. FRANTZ[2] and Y.-G. ZHANG[3]

[1]CREGU, B.P. 23, F-54500-Vandœuvre-lès-Nancy Cedex, France
e-mail: dubessy@cregu.cnrs-nancy.fr
[2]Geophysical Laboratory (CIW), 5251 Broad Branch Road NW, 20015-1305 Washington D.C., USA
[3]Institute of Geology, P.O. Box 9825, Beijing 100029, China
*Present address: LASIR, UER de Chimie, C8, F-59655-Villeneuve d'Ascq Cedex, France

Abstract: Raman spectra of fluids of the CO_2-CH_4-H_2O and CO_2-H_2O systems contained in synthetic fluid inclusions have been obtained above the homogenization temperature to 500°C. Spectra of the CO_2 and CH_4 gases do not vary along the portion of the studied isochore, whereas they do for the symmetric stretching band of water. The spectra clearly show that molecular interactions are stronger between CO_2 and H_2O molecules than between CH_4 and H_2O molecules. Gas molecules decrease the signature of hydrogen bonding in the Raman spectrum of water. For water-rich fluids, the ratio of Raman scattering cross-section of CH_4 and H_2O does not vary to a wide extent, showing that the calibration of this ratio is feasible.

Key-words: H_2O-CO_2-CH_4 system, Raman spectroscopy, synthetic fluid inclusions, molecular interactions, fluid-inclusion analysis.

Introduction

Water, the main component of crustal fluids, is also known as the fluid with the highest number of "anomalous" physical properties (Stillinger, 1980). These anomalous properties are the result of hydrogen bonds which give rise to a structure similar to that of a hydrogen bonded "transient gel" for liquid water at room temperature. Hydrogen bonds and their connectivity decrease with increasing temperatures. However, Raman spectroscopic works (Ratcliffe & Irish, 1982; Kohl *et al.*,1991; Frantz *et al.*, 1993), infrared experiments (Frank & Roth, 1967; Valyashko *et al.*, 1980; Bondarenko & Gorbaty, 1991; Gorbaty & Kalinichev, 1995), NMR studies (Nakahara, 1995), X-ray diffraction (Narten *et al.*, 1967; Gorbaty & Demaniets, 1983), neutron diffraction (Postorino *et al.*, 1994) and computer simulations (Kalinichev & Heinzinger, 1992, 1995; Kalinichev & Bass, 1994; Svishchev & Kusalik, 1995) document that hydrogen bonds and related structure still exist at temperatures as high as 400–500°C.

Water is not the sole molecular species present in deep geological fluids. Analysis of geothermal systems, fluid inclusions from hydrothermal and metamorphic environments, thermodynamic calculations of carbon or carbonate-bearing systems document fluids with CO_2, CH_4, N_2 and H_2, which are non dipolar molecules (NPM). NPM have weak attractive interactions with water molecules and NPM species must insert between the transient network of hydrogen bonds at room temperature, which is entropy producing and explains the low solubility of NPM molecules at room temperature. In addition, the weak attraction between

0935-1221/99/0011-0023 $ 2.50

Table 1. Properties of synthetic fluid inclusions. Composition in mole fraction X(i), molar volume (v), bulk homogenization temperature (Th (°C)) and phase of homogenization (L, liquid; V, vapour).

sample	$X(CO_2)$	$X(CH_4)$	$X(H_2O)$	v ($cm^3 \cdot mol^{-1}$)	Th (°C).
COH 94	0.055	0.057	0.888	29.5	328 (L)
1B	0.4725	0.000	0.5275	37.8	360 (V)
5A	0.711	0.000	0.289	45.72	308 (V)
2A	0.111	0.000	0.889	30.15	278 (L)
COH 99	0.055	0.105	0.84	47.78	365 (V)

water and NPM accounts for the topology of the critical curve starting from the critical point of water and moving to high pressure, a feature at the origin of an extended two-phase field. Increasing temperature disrupts hydrogen bonds and facilitates the insertion of NPM and therefore increases their solubility. The static dielectric constant of water-NPM strongly decreases with NPM concentrations at constant P and T, indicating a decrease in orientation correlation between water molecules (Deul, 1984; Franck, 1985).

Since Raman spectroscopy of water stretching (ν_2) vibration is sensitive to hydrogen bonding, the aim of this paper is to characterize the modifications of the Raman spectrum of water by NPM and to give preliminary interpretations in terms of molecular interactions. In addition, the intensity ratio of the Raman bands of the water-stretching vibration mode and of NPM molecules is examined in the perspective of fluid-inclusion analysis above the homogenization temperature by micro-Raman spectroscopy. Indeed, such approach might be the proper method to determine the bulk composition and density properties of natural fluid-inclusions since it will avoid the use of the inaccurate estimation of volume proportions of each phase at room temperature.

Density and temperature are the two parameters that control molecular interactions in a given system and therefore, *in situ* studies of isochoric systems, are more relevant than isobaric ones with respect to molecular interactions. Synthetic fluid inclusions are isochoric systems with known composition and density and are therefore adequate for the separation of density and temperature effects. Furthermore, the scattering geometry used for fluid inclusions is not similar to the scattering geometry used with a classical spectroscopic cell. Therefore, results obtained from synthetic fluid inclusions can be used for the analysis of natural fluid inclusions.

Sample preparation and experimental techniques

Synthetic inclusions in the H_2O-CO_2 system were prepared by the classical technique (Bodnar & Sterner, 1987). A mixture of H_2O and CO_2 was obtained from distilled H_2O and decomposed $Ag_2C_2O_4$. The H_2O-CO_2-CH_4 synthetic fluid inclusions used in this study are the ones described by Zhang & Frantz (1992), which were made using the gas-loading techniques (Frantz *et al.*, 1989). The composition and calculated molar volume and density of synthetic fluid inclusions are given in Table 1. The choice of inclusions was made in order to compare water-rich and water-poor inclusions, the influence of the nature of the gas (CO_2 or CH_4: 1B-5A *versus* COH 94, COH 99, 2A) at identical water content (2A *versus* COH 94) and fluids with liquid-like and vapour-like density (COH 94 *versus* COH 99).

Raman spectra were obtained with a Raman micro-spectrometer of a new generation (Labram, ®Dilor) equipped with a heating stage ®Chaixmecca). The high luminosity of the spectrograph and the CCD detector allow the acquisition of high-quality spectra within a few seconds. The high luminosity of the spectrometer is partially due to the use of Notch filter which remove radiations below 150 cm^{-1} from the exciting radiation λ_0 = 514.5 nm, 500 mW laser power from an ionized Ar^+ laser, ®Spectraphysics) in replacement of a fore-monochromator. Gratings have 1800 grooves per millimetre and the width of the spectral window is 1500 cm^{-1}. The spectral resolution constrained both by the aperture of the entrance slit (200 µm) and the distance between two pixels of the CCD detectors is 2 cm^{-1}. The precision in wavenumber, constrained by the number of pixel of the CCD is 1 cm^{-1}. Cold water flowing through a copper tube, wound around the long-working-distance objective (×80, 0.75 n.a., ®Olympus),

allowed acquisition of spectra to 500°C without producing any damage to the objective.

Results

A typical Raman spectrum obtained from a synthetic fluid inclusion at 429°C is illustrated in Fig. 1. At low wavenumbers, the weak bands of the quartz host crystal are identified, but do not overlap with the bands of the molecular compounds.

Description of the spectra of each component

Methane exhibits four Raman active bands, respectively the intense symmetric stretching mode (ν_1 = 2917 cm^{-1} for the isolated molecule at room temperature) and the very weak antisymmetric stretching band (ν_2 = 3006 cm^{-1} for the isolated molecule) and the weak overtones ($2\nu_4$ = 2576 cm^{-1} and $2\nu_2$ = 3070 cm^{-1}), which were all identified in the spectra (Fig. 1) (Herzberg, 1968). Within the precision of the measurements, the wavenumber and full width at half maximum intensity (FWHM) of the ν_1 band are constant composition and density (Fig. 2a, b) but has a value (ν_1 around 2911 cm^{-1}) lower than that of the isolated molecule. The FWHM of the ν_1 band is constant with temperature (around 10 cm^{-1}) and is higher for sample COH 94 homogenizing to the liquid state than for sample COH 99 homogenizing to the vapour state.

For carbon dioxide (Fig. 1), let us describe first the Raman spectrum obtained of the water-poor inclusion 5A at 383°C (Fig. 3c), which lost preferentially its water content during partial decrepitation, as already described by Bakker & Jansen (1992, 1994). Although only two bands are expected, the Raman spectrum 5A obtained at 383°C exhibits six bands as results of the Fermi resonance. These four additional bands, respectively at 1251, 1267, 1410, 1425 cm^{-1}, are called hot bands because they result of two effects (Finsterhölzl, 1982; Wienecke *et al.*, 1986): 1) the anharmonicity of the vibrational levels producing different energetic differences between two successive vibrational levels (E[v = 2] − E[v = 1] ≠ E[v = 1] − E[v = 0]); 2) the population of the excited vibrational levels which increases with temperature according to the Boltzman law. The Fermi resonance doubles the number of hot bands and explains their location on each side of the fundamental bands, at 1287 and 1388 cm^{-1}.

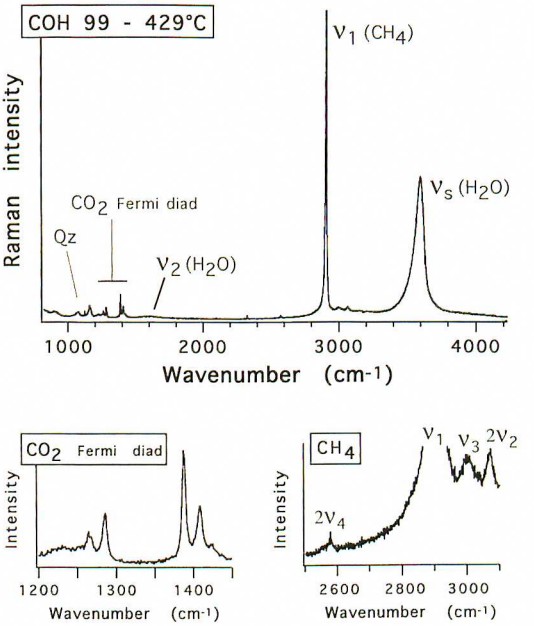

Fig. 1. Raman spectrum of fluid inclusion COH 99 obtained at 429°C.

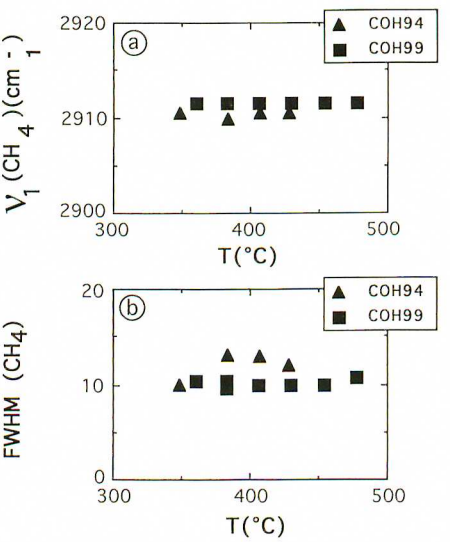

Fig. 2. Variation of the wavenumber and full width at half maximum intensity of the symmetric stretching mode (ν_1) of methane in methane-bearing H_2O-rich fluid *versus* temperature for two fluid compositions and densities.

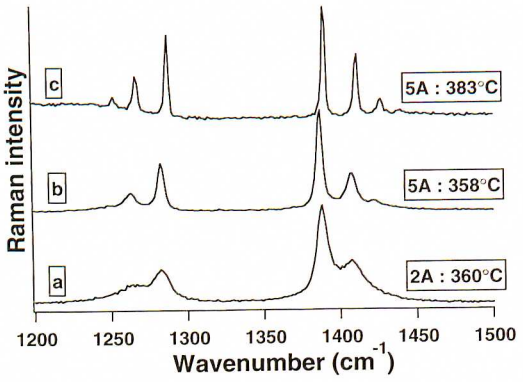

Fig. 3. Raman spectrum of carbon dioxide for different fluid compositions. a, 2A: $X(CO_2) = 0.111$; $X(H_2O) = 0.882$. b, 5A: $X(CO_2) = 7.11$; $X(H_2O) = 0.182$. c, 5A fluid inclusion after partial decrepitation at 383°C.

The addition of water modifies drastically the shape of spectra by enlarging the bands, as shown by comparison of spectrum 5A at 358°C (Fig. 3b) with the spectrum after decrepitation at 383°C (Fig. 3c). This band broadening increases with water content: 5A (358°C; Fig. 3b) and 2A (360°C; Fig. 3a). A more detailed analysis of the spectra was done by deconvoluting the spectra into different band components. The best fit was obtained for a band shape of 75% lorentzian and 25% gaussian (Fig. 4). Each band of the Fermi diad contains always three bands with wavenumber similar to the one obtained on water-poor carbon dioxide fluids. They are assigned to the fundamental and the hot bands of carbon dioxide molecule. It is worth noting that the high-intensity band components of the Fermi diad, obtained in our experiments, have higher wavenumbers (1282 –1285 cm^{-1} and 1386–1388 cm^{-1}) than those of carbon dioxide dissolved in water at room temperature (1274 cm^{-1} and 1382 cm^{-1}) or in clathrate molecules (1381 cm^{-1}) (Davis & Oliver 1972; Sze *et al.*, 1975; Anderson, 1977).

The FWHM of the hot bands are significantly higher than the FWHM of pure carbon dioxide but are always smaller than the values for carbon dioxide dissolved in water at room temperature or in clathrate molecules. Fitting the high-frequency massif of the Fermi diad into several components always requires an additional band between 1392 and 1407 cm^{-1}, which has a FWHM between 20 and 30 cm^{-1}, a value which is larger than the band components at 1286 and 1388 cm^{-1} for which 5<

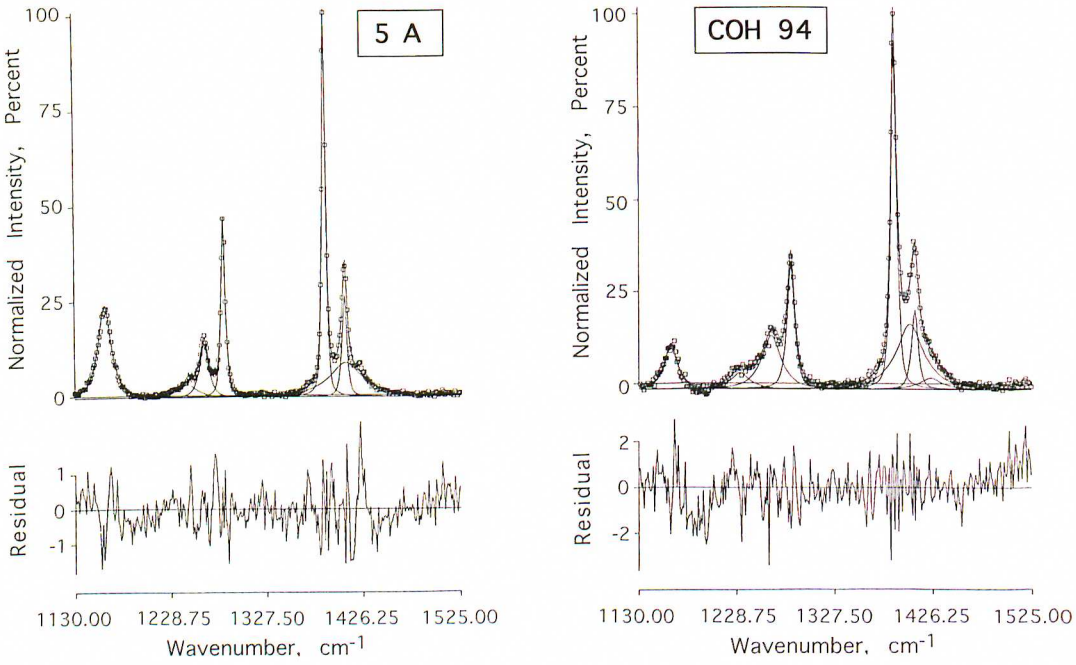

Fig. 4. Decomposition of the Raman spectrum of carbon dioxide from samples 5A (338°C) and COH 94 (364°C).

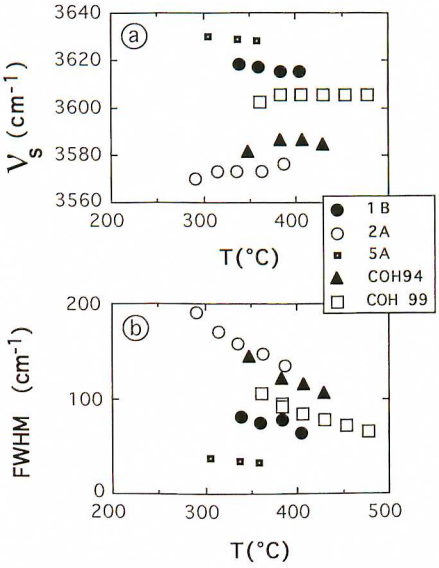

Fig. 5. a, Variation of the wavenumber at maximum intensity (ν_s) of the stretching band of water with temperature. b, Variation of the full width at half maximum intensity (FWHM) of the stretching band of water.

FWMM < 10 cm^{-1}. This band has no equivalent in pure CO_2 fluids and increases in intensity with increasing water content.

Water exhibits two bands assigned to internal motions, respectively the bending mode of water (ν_2) around 1600 cm^{-1} and a large massif assigned to stretching vibrations in the 3000–3800 cm^{-1} (Walrafen, 1964, 1967, 1972; Ratcliffe & Irish, 1982; Frantz *et al.*, 1993). The bending mode of water (ν_2) is weak and has not been studied in this work because of its small intensity (Fig. 1). The main effects of temperature on the Raman spectrum of pure water are the following (Ratcliffe & Irish, 1982; Frantz *et al.*, 1993): – the shift of the maximum intensity to high frequency (ν_s) with increasing temperature at constant density up to 250 °C and with decreasing density at constant temperatures above 250 °C; – the decrease in intensity of the band component around 3200 cm^{-1} resulting in a decrease of the FWHM of the whole stretching band. When compared with Raman spectra of other components, the Raman spectra of the stretching band of water is the one that exhibits the highest variations both in frequency at maximum intensity, FWHM and shape.

In H_2O-CO_2-CH_4 fluid mixtures, at constant temperature, the increase of molar volume at almost constant water concentration (COH 94, v = 29.5 cm^3·mole^{-1}; COH99, v = 47.78 cm^3·mole^{-1}) produces an increase of ν_s and a decrease of FWHM (Fig. 5). This effect is identical to the variations of these parameters observed in pure water at increasing molar volume (Frantz *et al.*, 1993). The highest values of ν_s and lowest values of FWHM are observed for the lowest water mole fraction 0.289 (5A) and 0.5275 (1B), *i.e.* for the highest NPM content (Fig. 5). Conversely, samples COH 94 ($X(H_2O)$ = 0.888) and 2A ($X(H_2O)$ = 0.889) have the lowest values of ν_s and highest values of FWHM. At almost constant molar volumes (COH 99; v = 47.78 cm^3·mole^{-1}; 5A, v = 45.72 cm^3·mole^{-1}), the decrease in water content ($X(H_2O)$ = 0.84 and $X(H_2O)$ = 0.289) results in an

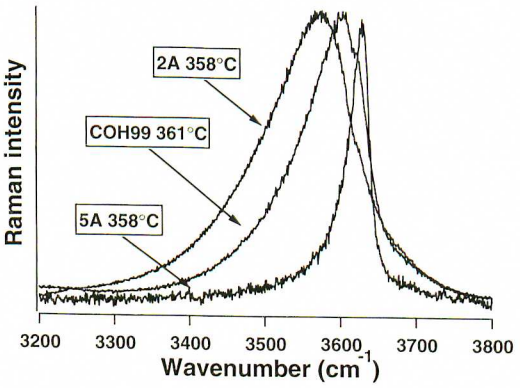

Fig. 6. Raman spectrum of the symmetric stretching mode of water in samples 2A [$X(H_2O)$ = 0.889], 5A [$X(H_2O)$ = 0.289] and COH 99 [$X(H_2O)$ = 0.84].

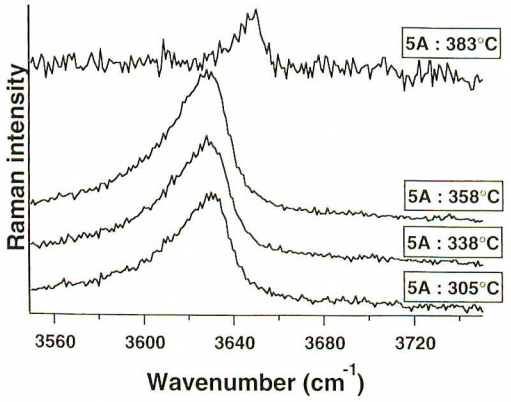

Fig. 7. Raman spectrum of the symmetric stretching mode of water in sample 5A before (305, 338 and 358 °C) and after partial decrepitation (383 °C).

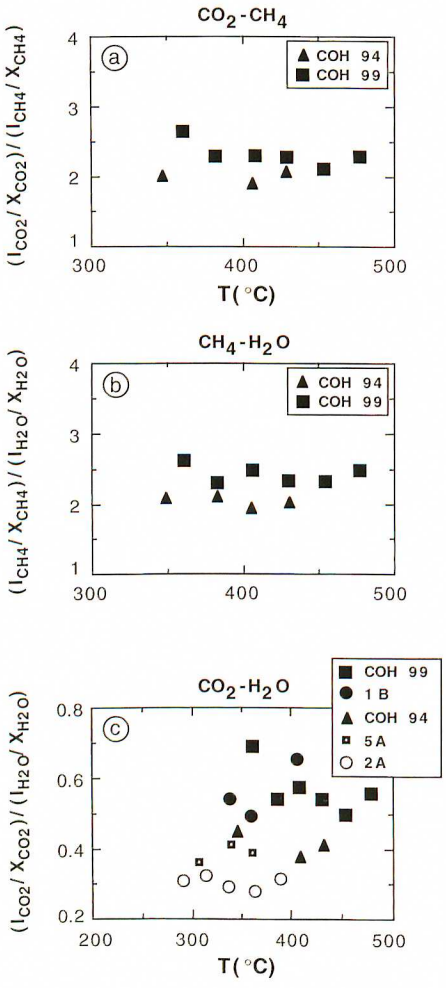

Fig. 8. Ratios of the intensity of Raman bands normalized with respect to the composition. a, CO_2-CH_4. b, CH_4-H_2O. c, CO_2-H_2O.

increase of ν_s and decrease of FWHM at the same temperature (Fig. 5 and 6). In addition, the type of NPM, CH_4 or CO_2-CH_4, at constant water concentration ($X(H_2O) = 0.89$) and molar volume (COH 94, v = 29.5; 2A, v = 30.15 $cm^3 \cdot mol^{-1}$) produces significant changes in the spectral features: ν_s increases and FWHM decreases when half of the CO_2 molecule is replaced by CH_4 molecules.

The variation of ν_s with temperature is of a few wavenumbers for the studied temperature range and the slope of this variation is positive for the most water-rich fluids COH 94 and 2A ($X(H_2O) = 0.89$) whereas it is negative for the water-poor fluids of vapour-like density (Fig. 5a). It is worth noting that ν_s of fluid COH 99 (water-rich and of vapour-like density) does not vary with temperature. In pure water, increasing temperature results always in an increase of ν_s at constant density (Frantz *et al.*, 1993). The FWHM decreases with increasing temperature: the higher the water content of the fluids, the larger the decrease (COH 94 and 2A, Fig. 5b). Water-rich fluids (COH 94 and 2A) with a density higher than the critical density at the considered composition display a weak band between 3200 and 3300 cm^{-1} as observed on the spectra of pure water (Frantz *et al.*, 1993). This low-frequency band is not detected in the spectra of fluid COH 99 which is water-rich and of vapour-like density.

Table 2. Comparison of the density and of the frequency at maximum intensity (ν_s) and FWHM of the Raman stretching band of gas-bearing aqueous fluids with the values obtained for pure water, noted H_2O* in this table (Frantz *et al.*, 1983).

samples	T (°C)	v ($cm^3 \cdot mol^{-1}$)	ν_s (cm^{-1})	FWHM (cm^{-1})
COH 94	349	29.50	3581	144
H_2O*	354	29.75	3575	125
1B	383	37.80	3615	78
H_2O*	376	37.58	3615	97
COH 99	454	47.78	3605	72
H_2O*	451	47.49	3617	72

The variations of ν_s and FWHM of inclusion 5A ($X(H_2O) = 0.289$) with increasing temperature along the isochore are small (Fig. 6). However, the spectrum of water obtained after partial decrepitation shows a strong increase of the ν_s value to 3650 cm^{-1}, very close to the value of the isolated water molecule (ν_s = 3655 cm^{-1}), and a decrease of FWHM to 5 cm^{-1} (Fig. 7). The band remains asymmetric with an enlargement towards the low frequency.

Comparison of the spectra of this work with those of pure water (Frantz *et al.*, 1993) obtained at the same temperature and for fluids with almost the same molar volume has been made on three sets of experiments (Table 2). The ν_s value of fluid COH 94 at 349 °C is higher than the corresponding value for pure water. However, its FWHM value is greater than the one obtained from the spectrum of pure water. For fluid 1B and its water equivalent, the ν_s values are identical but the FWHM of the pure water spectrum is much

higher. For fluid COH 99, the ν_s values of the gas-bearing fluid is smaller than the ν_s value of the pure water fluid, a reverse relationship from that observed between fluid COH 94 and its water counterpart.

Intensity ratios

The net integrated intensities of the Raman lines of each component were normalized with respect to composition by dividing them by the mole fraction of the considered component. For CO_2 the addition of the intensity of the two Fermi diads was made before normalization by composition. The ratios of the Raman normalized integrated intensities (RNII) were subsequently calculated for pairs of components. The CO_2-CH_4 RNII ratios do not vary significantly with temperature (Fig. 8a). Sample COH 99 has a CO_2-CH_4 RNII ratio of 0.23 and fluid COH 94 a CO_2-CH_4 RNII ratio of 0.20, indicating a small dependence with respect to composition and density. The CH_4-H_2O RNII ratios for one set of composition and density can be considered as constant along an isochore within the 350–500°C temperature range (Fig. 8b). The differences between samples COH 94 and COH 99 for CH_4-H_2O RNII ratios and CO_2-CH_4 RNII ratios are around 20%. The preliminary results indicate that the variations of the RNII ratios are small for fluids with vapour-like or liquid-like density and with water concentrations higher than 84 mol.%.

Ratios of RNII for CO_2-H_2O can also be considered to be constant as a function of temperature (Fig. 8c). RNII ratios between samples COH 99 and COH 94 vary between 0.43 and 0.56, a variation around 30% compared to a variation of 17% for CH_4-H_2O. Fluids 5A and COH 99 with similar molar volumes, respectively 45.72 and 47.78 $cm^3 \cdot mole^{-1}$, but very different water concentration have very different RNII ratios, demonstrating the influence of the water/gas ratio.

Discussion

Molecular interactions

The shift of an isotopic Raman band from its value at zero density is essentially attributed to two vibrational relaxation processes, the environmental fluctuations or vibrational dephasing, and the resonant transfer (Salmoun *et al.*, 1994). The low concentration of CH_4 makes the latter process inefficient for explaining the shift of the ν_1 mode of CH_4. The negative shift of 6–7 cm^{-1} shows that the attractive contribution is greater than the repulsive contribution and is significant. It is worth noting that this shift is close to the values found in methane clathrate, which exhibits two Raman bands, respectively at 2913 and 2903.5 cm^{-1} (Seitz *et al.*, 1987; Murphy & Roberts, 1995). The second important feature is the constancy of the value of ν_1 with increasing temperatures which documents that thermal agitation does not significantly weaken attractions between 300 and 500°C. Sample COH 99 with a molar volume higher than the critical molar volume has a ν_1 value higher than sample COH 94 with a molar volume smaller than the critical molar volume.

For CO_2, the negative shift towards low frequency is also essentially attributed to environmental fluctuations. This negative shift is smaller than that found for CH_4 because the Fermi resonance strongly modifies the response of frequency vibrations to molecular interactions. The two other vibrational modes of CO_2 are not Raman active, which precludes to use these modes as probe of molecular interactions.

The FWHM of the ν_1 of CH_4 is similar to that measured in pure methane fluid at room temperature (*i.e.* 3 cm^{-1} at a few bars and 5 cm^{-1} at 600 bars; Pasteris *et al.*, 1990). Both ν_1 and FWHM values and their variations suggest that molecular interactions of methane molecules in a water-rich fluid are not very strong. The FWHM of CO_2 bands is much more complicated to analyse. The fundamental bands at 1286 and 1388 cm^{-1} exhibit FWHM smaller than 10 cm^{-1}, indicating no line broadening with respect to pure CO_2. This contrasts with strong line broadening of the Fermi diads of CO_2 dissolved in water at room temperature, interpreted as coupling of the librational mode of H_2O at 685 cm^{-1} with ν_2 mode of CO_2 (Anderson, 1977). At the temperatures of our experiments, the thermal agitation is expected to weaken hydrogen bonds between water molecules and consequently also the coupling between libration of H_2O and ν_2 mode of CO_2. The broadening of hot bands remains unexplained.

The additional band around 1392–1407 cm^{-1} in the spectrum of CO_2 is tentatively considered to represent some strong interactions between carbon dioxide and water molecules and cannot be assigned to bicarbonate ion, characterised by bands at 1017 cm^{-1} (C-OH stretching vibration), 1302 cm^{-1} (C-OH bending vibration) and 1307 cm^{-1} (C=O

stretching vibration) (Davis & Oliver, 1972; Oliver & Davis, 1973), which all shift to low frequency at increasing temperature (Kruse & Franck, 1982). The weak band around 1010 cm^{-1} at 34° C-750 bars for 3 mol.% CO_2 in liquid water has been assigned to H_2CO_3 molecules by Kruse & Franck (1982) but has not been identified in our spectra. An equivalent additional component does not exist for methane. Is this band around 1392–1407 cm^{-1} representative of a stable chemical species or is it a solvation band? At this step, no firm interpretation can be done. It can only be recalled that the upper critical curve of the H_2O-CO_2 system shows a temperature minimum, in contrast to critical curves of the H_2O-CH_4 system, an indication of strong attraction between water and carbon dioxide molecules which are probably favoured by the quadrupole moment of carbon dioxide. It is worth noting that comparison of the water-stretching Raman band of fluids COH 94 and 2A, with the same water content and molar volume but with different CH_4/CO_2 ratio, indicates that the stretching vibration of water is affected by stronger pertubations in the presence of CO_2 than in the presence of CH_4.

The stretching massif of water cannot be explained easily. The different behaviours of ν_s with increasing temperature show that the attractive and repulsive contributions to vibrational dephasing have a temperature response that depends on composition and density. Comparison of the ν_s and FWHM values of the mixtures studied in this work with those of pure water (Table 2) shows that the mechanisms that control the variations of ν_s and FWHM are different.

Intensity ratios

The RNII ratio for CH_4-H_2O has been established on water-rich fluids for which each water molecule is statistically surrounded at least by 4 water molecules ($X(H_2O) > 0.84$). The differences found for the RNII ratio for CO_2 and CH_4 confirm that the Raman spectrum of these molecules are differently affected by their environment. The range of variations of the RNII ratios for CO_2-H_2O is higher than the range of variations found for CH_4-H_2O because the range of water/gas ratio is higher for the CO_2-H_2O system. Calibration of RNII ratios as a function of density for H_2O-rich fluids is probably sufficient and feasible for an analytical purpose. The comparison of fluids 2A and COH 94 shows also that the ratios of RNII for CO_2-H_2O depend on the CO_2/CH_4 ratio, even if water concentration and molar volumes are equal for the two samples. The application of Raman spectrometry to fluid-inclusion analysis above the homgenization temperature will require extensive experimental data. These results suggest that the bending mode of water (ν_2), which is known to exhibit much smaller variations for pure water as a function of pressure and temperature (Ratcliffe & Irish, 1982), should be investigated for checking its potential use in fluid-inclusion analysis.

Conclusion

Raman spectra of synthetic fluid inclusions in the CO_2-CH_4-H_2O and CO_2-H_2O systems have been obtained above the homogenization temperature to 500°C. The massif of the stretching vibration of water between 3000 and 3800 cm^{-1}, the Fermi diad of carbon dioxide and the symmetric stretching mode of methane have been investigated.

Wavenumber, shape and full width at half maximum of the Raman bands of CO_2 and CH_4 molecules do not vary along the studied portion of the isochore in contrast to those of H_2O molecules. This is interpreted by the fact that molecular interactions between H_2O molecules are mainly controlled by hydrogen bonding, which is very sensitive to temperature in a system with constant density and composition. The CO_2 and CH_4 molecules modify the Raman spectrum of H_2O indicating weaker hyrogen bonding. The wavenumber, shape and full width at half maximum of the Raman bands document that molecular interactions are stronger between CO_2 and H_2O molecules than between CH_4 and H_2O molecules. For water-rich fluids, the ratio of Raman scattering cross-section of CH_4 and H_2O does not vary to a wide extent, showing that the calibration of this ratio is feasible for an analytical purpose.

Acknowledgements: The work was supported by C.N.R.S. PICS no. 412. This manuscript benefited from the constructive comments of D. Irish and Y. Garrabos and from the reviews by B. Reynard and H. Keppler.

References

Anderson, G.R. (1977): The Raman spectra of carbon dioxide in liquid H_2O and D_2O. *J. Phys. Chem.*, **81**, 273–276.

Bakker, R.J. & Jansen, J.B.H. (1992): Experimental post-entrapment water loss from synthetic CO_2-H_2O inclusions in natural quartz. *Geochim. Cosmochim. Acta*, **55**, 2215–2230.

– – (1994): A mechanism for preferential H_2O leakage from fluid inclusions in quartz based on TEM observations. *Contrib. Mineral. Petrol.*, **116**, 7–20.

Bodnar, R. & Sterner, M. (1987): Synthetic fluid inclusions. *in* Hydrothermal Experimental Techniques. Barnes, H.L. & Ulmer, G.C., eds. Wiley and Sons, 423–467.

Bondarenko, G.V. & Gorbaty, Yu.E. (1991): An infrared study of water vapour in the temperature range 573–723 K. Dimerization enthalpy and absorption intensities for monomer and dimer. *Molecular Physics*, **74** (3), 639–647.

Davis, A.R. & Oliver, B.G. (1971): A vibrational spectroscopic study of the species present in the CO_2-H_2O system. *J. Sol. Chem.*, **1**, 329–339.

Deul, R. (1984): Dielectric constant and density of water-benzene mixtures to 400°C and 3000 bars. Unpubl. thesis, Institute for Physical Chemistry, Karlsruhe University.

Finsterhölzl, H. (1982): Raman sepctra of carbon dioxide and its isotopic variants in the Fermi Resonance Region: Part III. Analysis of rovibrational intensities for $^{12}C^{16}O_2$, $^{13}C^{16}O_2$, $^{12}C^{18}O_2$, and $^{12}C^{16}O^{18}O$. *Ber. Bunsenges. Phys. Chem.*, **86**, 797–805.

Franck, E.U. (1985): Aqueous mixtures to supercitical temperatures and high pressures. *Pure Appl. Chem.*, **57**, 1065–1070.

Franck, E.U. & Roth, K. (1967) Infrared absorption of HDO in water at high pressures and temperatures. *Discuss. Faraday Soc.*, **24–26**, 133–140.

Frantz, J.D., Dubessy, J., Mysen, B. (1993): An optical cell for Raman spectroscopic studies of supercritical fluids and its application to the study of water to 500°C and 2000 bars. *Chem. Geol.*, **106**, 9–26.

Frantz, J.D., Zhang, Y.G., Hickmott, D.D., Hoering, T.C. (1989): Hydrothermal reactions involving equilibrium between minerals and mixed volatiles. 1. Techniques for experimentally loading and analysing gases and their application to synthetic fluid inclusions. *Chem. Geol.*, **76**, 57–70.

Gorbaty, Y.E. & Demaniets, Y.N. (1983): The pair-correlation functions of water at a pressure of 1000 bars in the temperature range 25–500°C. *Chem. Phs. Lett.*, **100**, 450–454.

Gorbaty, Yu.E. & Kalinichev, A.G. (1995): Hydrogen bonding in supercritical water. 1. Experimental results. *J. Phys. Chem.*, **99**, 5336–5340.

Herzberg, G. (1968): Molecular spectra and molecular structure. II. Infrared and Raman spectra. Van Nostrand, London, 632 p.

Kalinichev, A.G. & Bass, J.D. (1994): Hydrogen bonding in supercritical water: a Monte Carlo simulation. *Chem. Phys. Letters*, **231**, 301–307.

Kalinichev, A.G. & Heinzinger, K. (1992): Computer simulations of aqueous fluids at high temperatures and pressures. *in* Advances in physical geochemistry, vol. **10**. Thermodynamic data: systematics and estimation. Saxena, S.K., ed. Springer-Verlag, Berlin, 1–59.

– – (1995): Molecular dynamics of supercritical water: a computer simulation of vibrational spectra with the flexible BJH potential. *Geochim. Cosmochim. Acta*, **59**, 641–650.

Kohl, W., Lindner, H.A., Franck, E.U. (1991): Raman spectra of water to 400°C and 3000 bar. *Ber. Bunsenges. Phys. Chem.*, **95**, 1586–1593.

Kruse, R. & Franck, E.U. (1982): Raman spectra of hydrothermal solutions of CO_2 and $KHCO_3$ at high temperatures and pressures. *Ber. Bunsenges. Phys. Chem.*, **86**, 1036–1038.

Murphy, P.J. & Roberts, S. (1995): Laser Raman spectroscopy of differential partitioning in mixed-gas clathrates in H_2O-CO_2-N_2-CH_4 fluid inclusions. *Geochim. Cosmoschim. Acta*, **59**, 4809–4824.

Nakahara, M. (1995): NMR studies on the effect of temperature and pressure on the structure and dynamics of aqueous systems. *in* Physical Chemistry of Aqueous Systems – Meeting the Needs of Industry. Proceedings of the 12th International Conference on the Properties of Water and Steam. White, H.J., Sengers, J.V., Neumann, D.B., Bellows, J.C., eds. Begell House, New York, Wallingford (U.K.), 449–459.

Narten, A.H., Danford, M.D., Levy, H.A .(1967): X-ray diffraction study of liquid water in the temperature range 4–200°C. *Discuss. Faraday Soc.*, **42**, 97–107.

Oliver, B.G. & Davis, A.R. (1973): Vibrational spectroscopic studies of aqueous alkali metal bicarbonate and carbonate solutions. *Can. J. Chem.*, **51**, 698–702.

Pasteris, J.D., Seitz, J.C., Wopenka, B., Chou, I.-M. (1990): Recent advances in the analysis and interpretation of C-O-H-N fluids by application of laser Raman microspectroscopy. *in* Geiss, R.H., ed. Microbeam Analysis, San Francisco Press Inc., San Francisco, 228–234.

Postorino, P., Ricci, M.-A., Soper, A.K. (1994): Water above its boiling point: study of the temperature and density dependence of the partial pair correlation functions. I. Neutron diffraction experiment. *J. Chem. Phys.*, **101**, 4123.

Ratcliffe, C.I. & Irish, D.E. (1982): Vibrational studies of solution at elevated temperatures and pressures, 5. Raman studies of liquid water up to 300°C. *J. Phys. Chem.*, **86**, 4897–4905.

Salmoun, F., Dubessy, J., Garrabos, Y., Marsault-Herail, F. (1994): Raman spectra of H_2S along the liquid-vapour coexistence curve. *J. Raman Spectrosc.*, **25**, 281–287.

Seitz, J.C., Pasteris J.D., Wopenka B. (1987): Characterization of CO_2-CH_4-H_2O fluid inclusions by microthermometry and laser Raman spectroscopy: inferences for clathrate and fluid equilibria. *Geochim. Cosmochim. Acta*, **51**, 1651–1664.

Stillinger, F.H: (1980): Water revisited. *Science*, **209**, 451–457.

Svishchev, I.M. & Kusalik, P.G. (1995): Spatial structure in liquid water under normal and critical conditions. *in* Physical Chemistry of Aqueous Systems – Meeting the Needs of Industry. Proceedings of the 12th International Conference on the Properties of Water and Steam. White, H.J., Sengers, J.V., Neumann, D.B., Bellows, J.C., eds. Begell House, New York, Wallingford (U.K.) 222–228.

Sze, Y.K., Adams, W.A., Davis A.R. (1975): A laser Raman study of clathrate hydrate and aqueous solutions of carbon dioxide. Proceedings of the Electrochemical Society Symposium on the Chemistry and Physics of Aqueous gas Solutions (Toronto, May 1975), 42–58.

Valyashko, V.M., Buback, M., Franck, E.U. (1980): Infrared absorption of concentrated aqueous LiCl solutions to high pressures and temperatures. *Z. Naturforsch.*, **35a**, 545–555.

Walrafen, G.E. (1964): Raman spectral studies of water structure. *J. Chem. Phys.*, **40**, 3249–3256.

– (1967): Raman spectral studies of the effects of temperature on water structure. *J. Chem. Phys.*, **47**, 114–126.

– (1972): Raman and infrared spectral investigations of water structure. *in* Water, a comprehensive treatise. Vol. **1**, The physics and physical chemistry of water. Frank, F., ed. Plenum Press, 151–214.

Wienecke, P., Finsterhölzl, H., Schrötter, H.W., Brandmüller, J. (1986): Raman spectra of carbon dioxide and its isotopic variants in the Fermi Resonance Region. Part IV: temperature dependence on Q-branch intensities from 300 K to 650 K. *Appl. Spectrosc.*, **40**, 70–75.

Zhang, Y.G. & Frantz, J.D. (1992): Hydrothermal reactions involving equilibrium between and mixed volatiles. 2. Investigations of fluid properties in the CO_2-CH_4-H_2O system using synthetic fluid inclusions. *Chem. Geol.*, **100**, 41–72.

Received 5 May 1997
Modified version received 8 December 1997
Accepted 30 July 1998